ELSEVIER

PII S0142-9612(97)00018-5

Biomaterials **18** (1997) 969–978

0142-9612/97/$17.00

Biomechanical characterization of osseointegration during healing: an experimental *in vivo* study in the rat

Rickard Brånemark*†‡, Lars-Olof Öhrnell*‡, Peter Nilsson§ and Peter Thomsen‡

*The Institute for Applied Biotechnology, Göteborg, Sweden; †Department of Orthopaedics, Sahlgren Hospital, Göteborg University, S-41345 Göteborg, Sweden; ‡Institute of Anatomy and Cell Biology, Göteborg University, Göteborg, Sweden; §Department of Oral and Maxillofacial Surgery, Göteborg University, Göteborg, Sweden

This study reports torsion tests and pull-out tests on osseointegrated commercially pure titanium fixtures. The tests were performed *in vivo* on a total of 26 rats. Three fixtures with a diameter of 2.0 mm were installed bilaterally in the proximal tibia in each animal. The mechanical testing was performed immediately after installation, after 2, 4, 8 and 16 weeks of unloaded healing. The torsional strength started to increase after 4 weeks of unloaded healing and there was a significant increase with time during the initial 16 weeks. The pull-out load increased rapidly during the first 4 weeks; thereafter, a moderate increase occurred during the following 12 weeks. A histological evaluation was performed after 0, 4, 8 and 16 weeks. There were significant ($P < 0.01$) correlations between torque and percentage of bone in contact with the fixture, and between pull-out load and the bone thickness around the fixture ($P < 0.001$). Estimations of shear stresses and shear moduli in the bone tissue (pull-out test) and at the interface (torque test) indicated that the increase in bone volume around the implant substantially improved the mechanical capacity.

Keywords: Titanium, osseointegration, implants, biomechanics, healing, bone

Accepted 11 January 1997

Osseointegrated titanium implants (fixtures) have successful long-term clinical records in oral[1,2] and craniofacial surgery[3]. The fixtures are normally installed in the bone tissue in a first operation. Thereafter, they are left unloaded for healing during 3–6 months. In a second operation the fixtures are connected to a superstructure and loaded. It is assumed that an early postoperative period without load contributes to the structural and functional incorporation of fixtures in the bone. Increased knowledge about the early phase of healing may be of importance for understanding factors required for achieving osseointegration and to identify the optimal time of initial loading.

This study represents one part of a series of ongoing experimental and clinical investigations of the biomechanics of the interface between bone and implant. These investigations are performed in humans[4], beagles[5], rabbits[6] and rats[7] during normal and pathological conditions.

The aim of the present experimental study was to evaluate the biomechanics of titanium fixtures in the rat, after varying periods of unloaded healing, by *in vivo* torsion tests, pull-out tests and histological analysis.

Correspondence to Dr R. Brånemark, Department of Orthopaedics, Sahlgren Hospital, Göteborg University, S-413 45 Göteborg, Sweden.

MATERIAL AND METHODS

Animals

A total of 26 male, mature Sprague-Dawley rats, mean weight 350 g, were divided into five groups. Five animals were subjected to mechanical testing immediately after fixture installation, four animals after 2 weeks, five animals after 4 weeks, six animals after 8 weeks and six animals after 16 weeks. The experiments were approved by the Local Ethics Committee.

Surgical procedure

Threaded commercially pure titanium fixtures were manufactured by machining (diameter 2.0 mm; *Figure 1*). Ultrasonical cleaning in series of butanol and ethanol (10 min in each solution) was followed by sterilization by autoclaving. The animals were anaesthetized by intraperitoneal injections of barbiturates and benzodiazepines. After shaving and washing of both hind legs, surgery was performed under sterile conditions.

Special care was taken to assure that the prerequisites for achieving osseointegration were fulfilled[1]. The medial aspect of the proximal tibial metaphysis was exposed through an antero-medial skin incision. With a series of drill guides and burrs (*Figure 1*), three fixtures were installed in a straight line. Profuse irrigation with room temperature saline was used to avoid heat

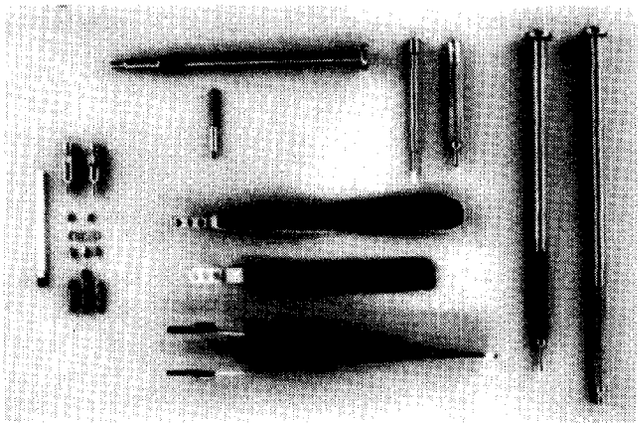

Figure 1 The fixtures and the surgical equipment used.

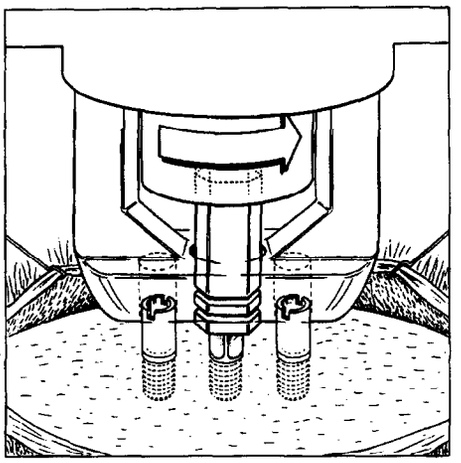

Figure 2 Schematic of the torsion test set-up.

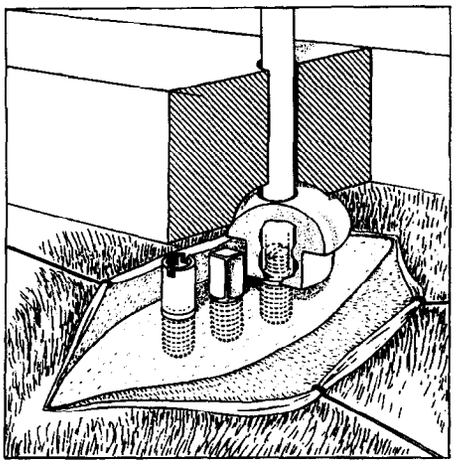

Figure 3 Schematic of the pull-out test with the hemisphere in place.

production that could damage the bone tissue. The drilled holes were tapped manually. The side fixtures had threaded heads and the central fixture had a square head. The centre-to-centre distance between the fixtures was 4.5 mm. To prevent movements of the fixtures during the healing period, the three fixtures were connected to each other by a thin titanium plate fixed by cover screws to the side fixtures and by press-fit of a square-hole onto the square-headed central fixture. Soft tissues were mobilized to cover the fixtures. The wound and skin was closed in layers with absorbable sutures (Dexon®, Davis-Geck, Cyanamid Medical Device Co Inc., Anyang, Korea). The wound region was protected with a topical wound dressing (Nobecutane, Apoteksbolaget, Umeå, Sweden). The procedure was carried out bilaterally. Postoperatively, the animals were allowed to move freely.

Procedure during the mechanical tests

After the healing period, the *in vivo* mechanical testing was performed. The animals were again anaesthetized as described above. After surgical exposure the cover screws and the positioning plate were removed. Careful dissection was performed to avoid any load being applied to the fixtures during the removal of soft tissues covering the fixtures and in some instances newly formed bone tissue. Special abutments were connected to the side fixtures. These abutments fitted into a test equipment for torsion testing[8] (*Figure 2*). By the use of a special guide, torque could be applied to the square head of the central fixture (angular deformation rate $2° \text{ min}^{-1}$) without any pre-load. The test was terminated after the maximal torque was reached (normally within 40° of rotation). After the torque test the special abutments were disconnected and an internally threaded rod connected to the threaded head of the proximal side fixture. This rod was then attached to a pull-out test set-up[8]. A hemisphere with an internal hole (diameter 3.0 mm) was used to support the surrounding bone during the pull-out test (*Figure 3*). This construction reduces the influence of possible irregularities on the bone surface. The pull-out test was terminated shortly after the maximal load was reached (deformation rate 0.5 mm min^{-1}).

Histological preparation

Just before the animal was killed, the proximal section of the tibia with the three fixtures was removed *en bloc*, fixed in 2.5% glutaraldehyde and then postfixed in 2% osmium tetroxide for 1 h. After dehydration in a graded series of ethanol the specimens were embedded in a plastic resin (LR White, The London Resin Co Ltd, Hampshire, UK). The fixtures were divided longitudinally by sawing (Exact cutting and grinding equipment, Exact Apparate Bau, Norderstedt, Germany). Ground sections were prepared and stained with 1% toluidine blue. Only a limited number of fixtures were available for histological analysis due to technical problems.

Light microscopic morphometry was performed on the ground sections in a Leitz Metallux microscope connected to a Microvid computer system. The percentage of bone-to-metal contact and the bone area were measured within each thread of the central fixture subjected to torsion. The bone thickness was measured at 50 (t_{50}), 250 (t_{250}) and 550 (t_{550}) μm distances from the outer edge of the threads (*Figure 4*) on both sides of all fixtures, and the mean was calculated for each fixture as well as for the three fixtures in each leg for each animal.

Statistical methods

All statistical analyses were based on animals, not on legs or fixtures. For each animal the means over fixtures and legs were calculated and these means were then used in the statistical analyses. Pitman's non-

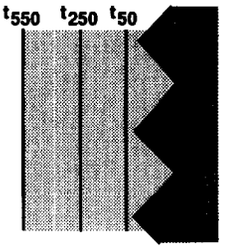

Figure 4 The bone thickness was measured at a distance of 50 μm (t_{50}), 250 μm (t_{250}) and 550 μm (t_{550}) from the outer edge of the threads of the titanium fixture (Ti), respectively.

parametric permutation test[9] was used for all correlation analyses. In addition, Pearson's correlation coefficient was calculated. The least square regression line was estimated and included in the scatter plots between mechanical tests and histology. The partial correlation coefficient was used to study the correlation between two variables adjusted for a third variable. For comparison between right and left sides, Fisher's non-parametric permutation test for matched pairs[9] was used.

RESULTS

In a total of 26 rats, 156 screw-shaped titanium fixtures were installed in the proximal tibia bilaterally. Healing occurred uneventfully after fixture installation in all animals. Torque tests were applied to 52 fixtures and pull-out tests to 52 fixtures. Histological analysis was performed in five animals immediately after fixture installation (30 fixtures), two animals after 4 weeks (12 fixtures), one animal after 8 weeks (6 fixtures) and four animals after 16 weeks (24 fixtures).

Mechanical tests

The torque and pull-out test results are summarized in *Figure 5* and *Table 1*. During the initial 4 weeks, the registered torque levels were unchanged. There was a significantly ($P < 0.001$) increasing torsional capacity from 4 to 16 weeks of healing. The pull-out load increased ($P = 0.016$) rapidly during the first 4

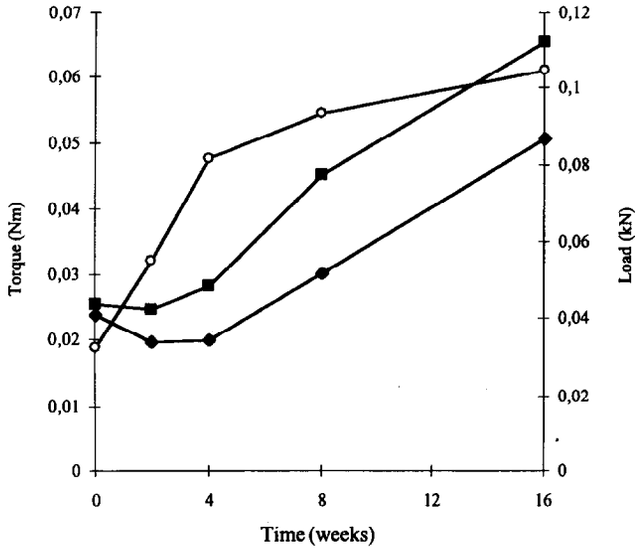

Figure 5 The effect of healing on torsion and pull-out load. ◆, Break point torque; ■, maximal torque; ○, pull-out load.

Table 1 Mean, range and sample size for mechanical and histomorphometric results, by healing time

	0 weeks	2 weeks	4 weeks	8 weeks	16 weeks
Mechanical results	$n = 5$	$n = 4$	$n = 5$	$n = 6$	$n = 6$
Break point torque (10^{-3} Nm)	24.0 (14.2–28.7)	19.9 (10.9–31.0)	20.0 (10.2–26.5)	30.4 (20.0–42.0)	50.8 (29.5–73.5)
Maximal torque (10^{-3} Nm)	25.7 (16.0–29.5)	24.8 (14.7–40.0)	28.4 (19.2–36.7)	45.2 (39.9–53.5)	65.5 (50.5–90.0)
Pull-out load (N)	32.6 (16.3–53.4)	55.2 (14.0–107.5)	81.5 (46.7–111.4)	93.4 (58.0–134.7)	104.8 (77.4–145.5)
Histomorphometric results	$n = 5$	$n = 0$	$n = 2$	$n = 1$	$n = 4$
Bone thickness t_{50} (μm)	556 (497–611)	—	1053 (916–1190)	1356	1164 (995–1442)
Bone thickness t_{250} (μm)	505 (437–552)	—	758 (663–853)	1007	845 (764–963)
Bone thickness t_{550} (μm)	495 (450–532)	—	698 (621–775)	947	781 (719–922)
Bone area (%)	24 (20–28)	—	43 (33–52)	55	55 (46–68)
Bone contact (%)	26 (21–37)	—	51 (45–58)	—	70 (60–81)
Shear stresses and shear moduli	$n = 5$	$n = 0$	$n = 2$	$n = 0$	$n = 4$
Pull-out shear stress (MPa)	11 (8–16)	—	15 (15–16)	—	16 (10–23)
Pull-out shear modulus (MPa)	24 (11–34)	—	25 (22–28)	—	45 (26–67)
Break point torque shear stress (MPa)	4.3 (2.6–5.5)	—	1.9 (1.7–2.0)	—	3.2 (2.4–3.9)
Maximal torque shear stress (MPa)	4.5 (3.0–5.7)	—	2.2 (1.9–2.4)	—	4.0 (3.5–4.4)
Torsional shear modulus, 100 nm (MPa)	0.006 (0.002–0.007)	—	0.004 (0.003–0.004)	—	0.00445 (0.003–0.006)
Torsional shear modulus, 1000 nm (MPa)	0.055 (0.021–0.065)	—	0.035 (0.030–0.041)	—	0.045 (0.030–0.062)

Table 2 Correlation analyses: mechanical tests–healing time–histology

	Healing time	Bone thickness t_{50}	Bone thickness t_{250}	Bone thickness t_{550}	Bone contact	Bone area
Break point torque	$r = 0.74$ ($P < 0.001$)	$r = 0.68$ ($P = 0.020$)	$r = 0.69$ ($P = 0.020$)	$r = 0.69$ ($P = 0.022$)	$r = 0.78$ ($P = 0.001$)	$r = 0.76$ ($P = 0.007$)
Maximal torque	$r = 0.87$ ($P < 0.001$)	$r = 0.76$ ($P = 0.007$)	$r = 0.77$ ($P = 0.008$)	$r = 0.78$ ($P = 0.007$)	$r = 0.85$ ($P = 0.004$)	$r = 0.85$ ($P = 0.002$)
Pull-out load	$r = 0.65$ ($P < 0.001$)	$r = 0.87$ ($P < 0.001$)	$r = 0.94$ ($P < 0.001$)	$r = 0.90$ ($P < 0.001$)	— —	— —
Healing time	— —	$r = 0.77$ ($P = 0.008$)	$r = 0.76$ ($P = 0.008$)	$r = 0.74$ ($P = 0.011$)	$r = 0.91$ ($P = 0.002$)	$r = 0.85$ ($P = 0.003$)

Pearson correlation coefficients and *P*-values obtained by Pitman's non-parametric permutation test.

weeks, whereafter a moderate non-significant increase occurred during the following 12 weeks. For correlations over the whole time span, 0–16 weeks, see *Table 2*. A schematic curve of applied torque versus angle of rotation is shown in *Figure 6*. Initially, there was an almost linearly rising torque up to a few degrees, whereafter a plateau region was reached with almost constant torque level, sometimes increasing slightly, but then gradually declining for increasing angles. The initial segment was nearly linear up to a small angle at which the slope decreased distinctly. This point of change of slope is called the 'break point' (*Figure 6*), as it is similar to the break point (or elastic limit) observed in torsion tests (or tensile tests) of circular cylindrical bars of metals. However, there is a difference in the behaviour of metals and the torsion test results reported here. If a metallic specimen is unloaded from a point below the elastic limit, it retraces the original loading curve and, if fully unloaded, returns to the origin of zero torque and zero angular displacement. In the torsion tests of fixture in bone reported here, when the torque was reduced from any point below or above the break point, it did not follow down the initial loading curve, but followed a steeper line (*Figure 6*), and at zero torque it did not return to the zero angular position. This residual, irrecoverable deformation is similar to the plastic deformation of metals. However, in metals such plastic deformation does not occur unless the loading is carried initially to a point beyond the elastic limit.

A schematic plot of pull-out load versus extensional displacement (extension) is illustrated in *Figure 7*. The initial linear portion of the curve extended up to a fairly well defined break point. The maximal load was

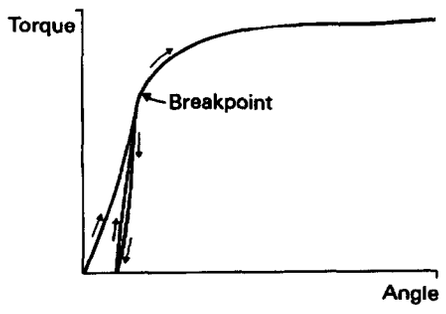

Figure 6 A schematic plot of applied torque versus angle of rotation. When unloading there is already, after a few degrees of rotation, a residual plastic deformation.

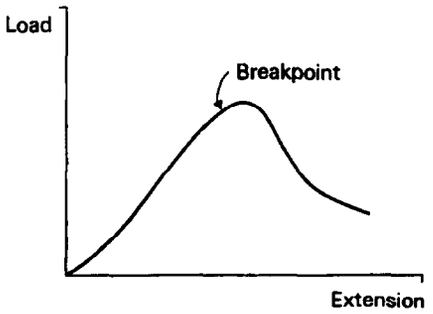

Figure 7 A schematic plot of pull-out load versus extension.

reached shortly beyond this break point, after which the load rapidly declined as the extension was increased. No statistically significant differences were found between the right and left sides for any of the mechanical tests (*Table 3*).

Histology

Light microscopic analysis of ground sections was performed on the specimens obtained immediately after insertion (0 weeks), and after 4, 8 and 16 weeks. As revealed by the 0 week specimens, the upper one or two threads of the fixture were located in the compact cortical layer of the tibia (*Figure 8a*). At this point of time the cut bone surface was in focal contact with the surface of these threads, and the space between the bone and the implant surface was occupied by erythrocytes. Fracture lines in the bone around the fixtures subjected to torque and pull-out were difficult to distinguish.

After 4 weeks, new bone formation was evident on both the endosteal, periosteal and cut, injured surfaces (*Figure 8b, d, f*). Prominent findings were endosteal down-growth together with extensive periosteal new bone formation of woven character with areas containing soft tissue where mineralization foci (islands of new bone formation) could be observed.

The histological observations after 8 and 16 weeks were similar, with mature compact bone, extending into the bone marrow, forming a collar-like pattern around the fixtures (*Figure 8c, e, g*). Large areas were found to undergo remodelling, with formation of new marrow-like cavities in the compacta. In comparison with the morphological observations after 4 weeks, a larger proportion of the threads were filled with

Table 3 Differences between right and left sides in torque, pull-out, histomorphometry, shear stresses and shear moduli

	n	Right side Mean (s.d.) Range	Left side Mean (s.d.) Range	Difference Right – left side Mean (s.d.) Range	*P*-values* Differences	Number where right side is lower
Mechanical tests						
Break point torque (10^{-3} Nm)	25	28.8(15.1) 5.0–56.7	31.1(18.9) 5.7–97.0	−2.3(13.6) −47.0–22.0	n.s. $P > 0.30$	12
Angle at break point torque (°)	25	4.0(2.4) 0.3–10.0	3.9(2.2) 0.8–8.5)	0.1(2.7) −4.5–7.0	n.s. $P > 0.30$	11
Maximal torque (10^{-3} Nm)	25	38.6(19.7) 14.3–83.0	39.8(19.6) 10.0–97.0	−1.3(11.5) −28.0–22.0	n.s. $P > 0.30$	14
Angle at maximal torque (°)	25	18.3(13.1) 4.3–44.0	17.6(11.9) 3.1–42.3	0.8(17.7) −37.9–39.3	n.s. $P > 0.30$	12
Pull-out load (N)	26	76.8(43.5) 18.7–165.3	75.5(39.2) 3.0–155.0	1.0(40.0) −102.0–89.0	n.s. $P > 0.30$	13
Extrusion (mm)	26	0.28(0.12) 0.14–0.66	0.28(0.12) 0.14–0.60	0.00(0.14) −0.26–0.36	n.s. $P > 0.30$	12
Histology (mean of all fixtures)						
Bone thickness t_{50} (μm)	12	864(317) 464–1391	952(385) 456–1513	−88(164) −422–98	n.s. $P < 0.10$	8
Bone thickness t_{250} (μm)	12	655(190) 403–1001	749(245) 434–1144	−94(190) −607–107	n.s. $P < 0.10$	9
Bone thickness t_{550} (μm)	12	609(152) 420–901	714(223) 422–1018	−105(164) −475–91	$P = 0.034$	9
Bone area (%)	12	38.3(14.0) 20.9–57.0	42.0(19.3) 18.3–78.5	−3.7(7.6) −21.5–5.0	n.s. $P = 0.12$	8
Bone contact (%)	11	42.7(20.2) 20.7–70.9	50.3(24.2) 20.3–90.2	−7.6(9.1) −27.5–2.4	$P = 0.01$	9
Shear stresses and shear moduli						
Pull-out shear stress (MPa)	11	14.5(5.5) 8.4–24.5	13.0(5.0) 5.2–22.3	1.5(5.2) −6.9–12.6	n.s. $P > 0.30$	4
Pull-out shear modulus (MPa)	11	33.8(18.2) 14.5–72.9	30.1(15.8) 4.9–62.0	3.7(11.5) −13.5–20.4	n.s. $P > 0.30$	4
Break point torque shear stress (MPa)	10	3.8(1.50) 1.8–6.2	3.3(1.3) 1.7–5.6	0.45(0.78) −0.64–2.09	n.s. $P < 0.10$	3
Maximal torque shear stress (MPa)	10	4.2(1.5) 2.1–6.5	3.7(1.3) 1.8–5.8	0.52(0.97) −0.45–2.26	n.s. $P = 0.13$	5
Torsional shear modulus, 100 nm (MPa)	10	0.0054(0.0021) 0.0025–0.0082	0.0045(0.0017) 0.0018–0.0067	0.00096(0.00191) −0.0014–0.0045	n.s. $P = 0.17$	4
Torsional shear modulus, 1000 nm (MPa)	10	0.054(0.021) 0.025–0.082	0.045(0.017) 0.018–0.067	0.0096(0.0191) −0.014–0.045	n.s. $P = 0.17$	4

*P-values calculated with Fisher's non-parametric permutation test for matched pairs.

compact bone and the surface was in contact with mature mineralized bone.

Morphometry

The results of the light microscopic morphometry are summarized in *Figure 9* and *Table 1*. The samples were evaluated with respect to the percentage of bone–implant contact (%bc), bone area within the threads (%ba) and the bone thickness 50 (t_{50}), 250 (t_{250}) and 550 μm (t_{550}) out from the fixture.

Immediately after insertion (0 weeks), there was a uniform bone thickness of about 500 μm around the fixture, irrespective of the distance from the fixture. During the healing period the bone thickness increased at all three measured distances (*Table 1*). The increase was greatest close to the fixture (t_{50}) and more pronounced from 0 to 4 weeks of healing than from 4 to 16 weeks (*Figure 9*). The percentage of bone–implant contact and bone area within the threads increased with time (*Table 1*).

The bone thickness t_{550} was significantly higher ($P < 0.05$) on the right side than on the left side. There was significantly ($P < 0.01$) less percentage bone contact on the right side compared to the left side (*Table 3*).

Correlations between mechanical tests and morphometry

It is expected from a mechanical viewpoint to find a correlation between mechanical data and histological data. Break point torque and maximal torque were significantly correlated to all histological data (*Table 2, Figures 11–14*). Pull-out load was significantly ($P < 0.001$) correlated to the bone thicknesses t_{50}, t_{250} and t_{550} (*Table 2* and *Figure 10*).

Partial correlation analyses were performed on break point torque and maximal torque, correlated to bone thickness and percentage bone contact, respectively. By eliminating percentage bone contact, no correlation was found between either break point torque or maximal torque and bone thickness. By eliminating t_{50} (taken as the mean for all fixtures and for the right and left sides), there was still a significant partial correlation ($r = 0.67$, $P = 0.033$) between maximal torque and percentage bone area, and a non-significant tendency ($r = 0.56$, $P = 0.09$)

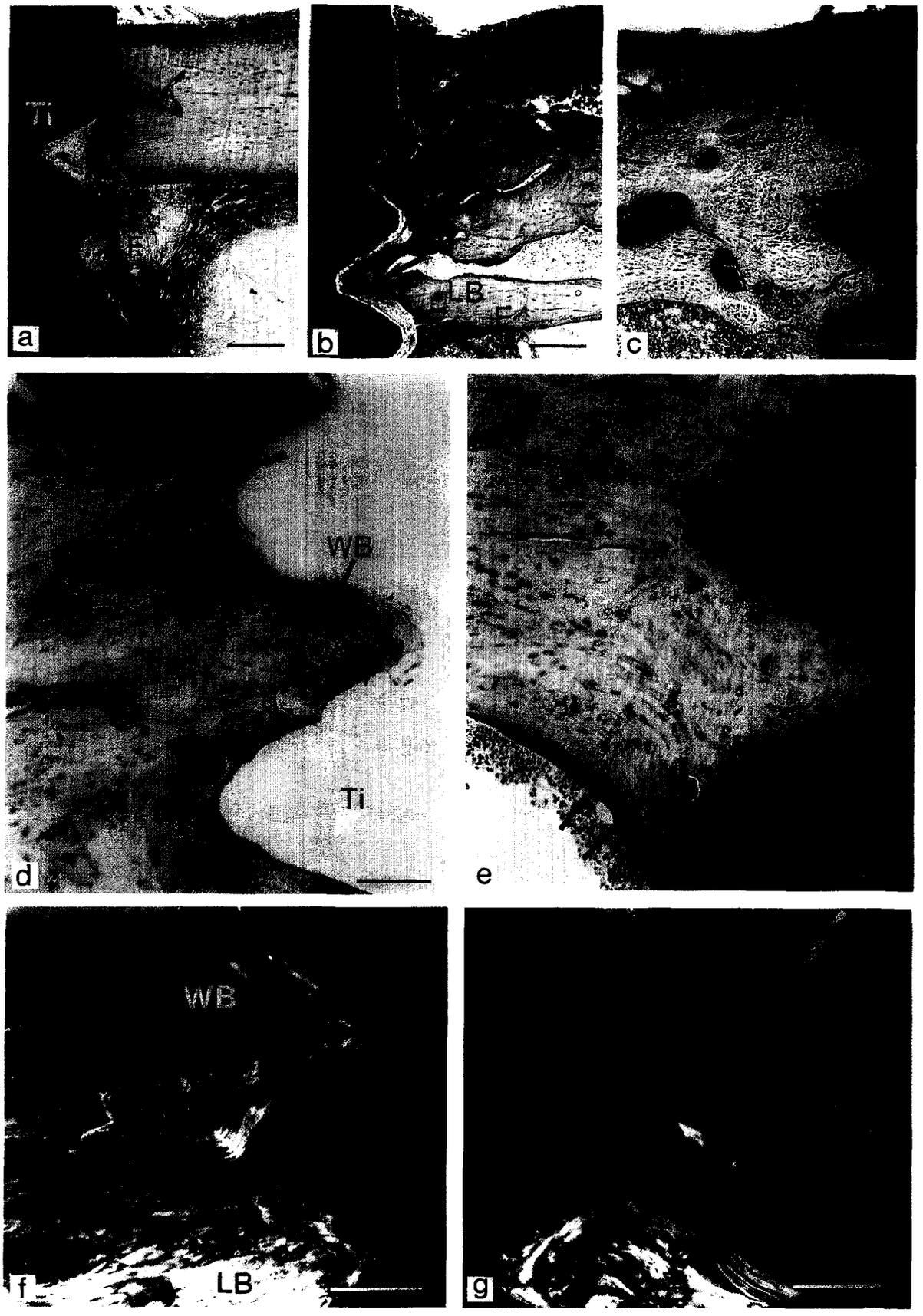

Figure 8 Light microscopy (LM) of bone around fixtures 0, 4 and 16 weeks after insertion in rat tibial bone. **a,** LM showing the location of a fixture in the cortical bone immediately after insertion (0 weeks). The area within threads is occupied by erythrocytes. Fragment (F) of endosteal lamellar bone is projecting into the marrow. Ti, titanium. Bar = 200 μm. **b,** LM survey of the bone–implant area 4 weeks after insertion. New woven bone (arrows) is observed within threads and in the periosteal (P) and endosteal (E) regions. A marked remodelling of bone is detected in the specimen. There is some old lamellar bone (LB). Bar = 200 μm. **c,** LM survey of the bone–implant area 16 weeks after insertion. Dense, compact bone occupies the areas within threads and in the periosteal (P) and endosteal (E) regions. Bar = 200 μm. **d,** LM of bone within threads in the cortical layer 4 weeks after insertion. Old lamellar bone (LB) undergoes resorption (arrowheads) in several areas. The central thread is occupied by lamellar bone, new woven bone (WB, arrow) and soft tissue (ST). The titanium implant was accidentally removed during ground sectioning. Bar = 100 μm. **e,** LM of bone which occupies and is in contact with the threads in the cortical layer 16 weeks after insertion. Bone down-growth from the endosteal area is observed (arrows). Bar = 100 μm. **f,** LM (polarized light) of specimen 4 weeks after insertion. Lamellar bone (LB) is not in contact with the surface of the fixture. Periosteal woven bone is present (WB). Bar = 150 μm. **g,** LM (polarized light) of specimen 16 weeks after insertion. Lamellar bone has formed in the periosteal (white arrows) and thread regions (black arrow). Bar = 150 μm.

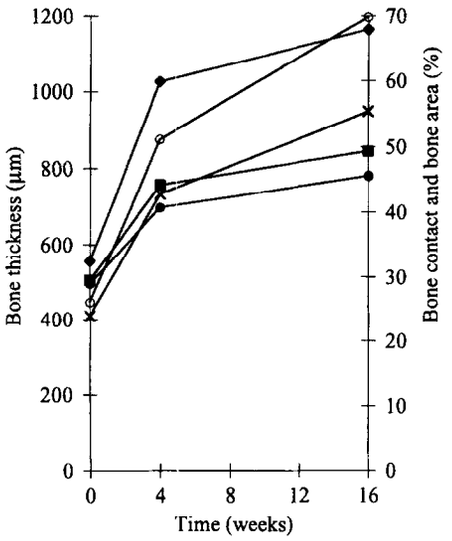

Figure 9 The effect of healing on histological parameters (see text). ◆, t_{50}; ■, t_{250}; ●, t_{550}; ×, bone area; ○, bone contact.

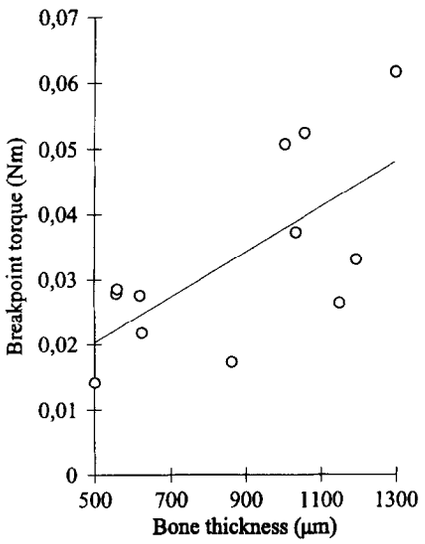

Figure 11 A scatter plot of break point torque versus bone thickness (at 50 μm distance from the outer edge of the thread): $r = 0.68$, $P = 0.020$, Pitman's test. A regression line was included.

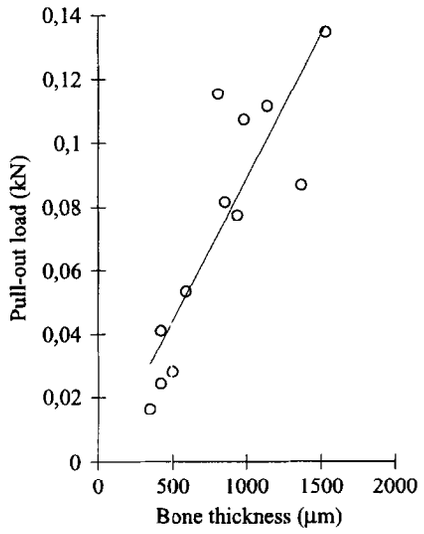

Figure 10 A scatter plot of pull-out load versus bone thickness (at 50 μm distance from the outer edge of the thread): $r = 0.87$, $P < 0.001$, Pitman's test. A regression line was included.

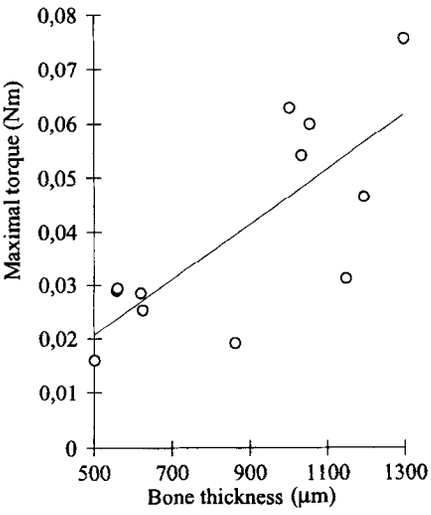

Figure 12 A scatter plot of maximal torque versus bone thickness (at 50 μm distance from the outer edge of the thread): $r = 0.76$, $P = 0.007$, Pitman's test. A regression line was included.

between maximal torque and percentage bone contact, indicating that bone tissue closer than 50 μm from the fixture surface has an influence on the mechanical torsional capacity.

Biomechanical considerations

The torsion test is assumed to be primarily probing the interface mechanics, because the fixture design will first transfer the stresses to the interface region, which is weaker than the intact bone.

In contrast to the torsion tests, the results of pull-out tests are assumed to be dependent more on the properties of the bone surrounding the implant and less on the properties of the interface. The implants are not assumed to be damaged in these tests and they will move as rigid bodies when deforming the surrounding bone. The fact that the pull-out tests are primarily testing the surrounding bone is due to the geometry of the implants. The threads constitute an efficient load transfer mechanism, from the fixture out to the surrounding bone, without the need to depend on generation of shear stresses in the interface region. From a theoretical viewpoint there should be a correlation between bone thickness and pull-out load. This assumption is supported by the results in the present study (*Table 2* and *Figure 10*).

It would be desirable to be able to relate measured loads directly to varying test geometries and amount, structure and distribution of the bone present around the fixtures. This will require detailed information on the density and distribution of the bone surrounding the fixtures, as well as detailed computation of stress distributions.

Some approximate average stress behaviour may be definable by simplified models. This is most obvious for the torsion test. Assuming that sliding occurs at the interface, an average shear stress can be accurately

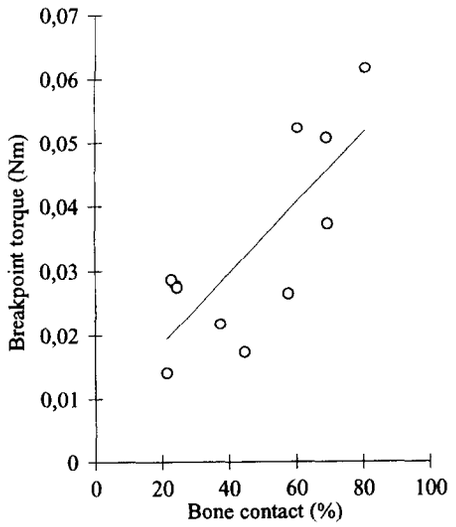

Figure 13 A scatter plot of break point torque versus percentage bone contact: $r = 0.78$, $P = 0.001$, Pitman's test. A regression line was included.

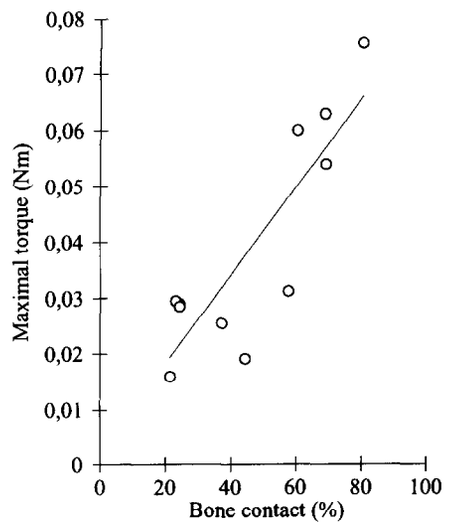

Figure 14 A scatter plot of maximal torque versus percentage bone contact: $r = 0.85$, $P = 0.004$, Pitman's test. A regression line was included.

computed for the screw as a whole. However, to be a useful criterion, it must be taken into account that only a certain percentage of the fixture area has a close apposition to bone. The geometrical distribution of the bone tissue can also be of importance. Is the mechanical capacity influenced by the thin layer of encapsulating bone? In the present study there was a significant correlation between bone thickness t_{50}, break point torque and maximal torque, respectively (*Table 2*, *Figures 11* and *12*). A stronger correlation was found between the degree of bone contact (%bc) and torsional capacity (*Figures 13* and *14*). This indicates that the encapsulating bone has the capacity to take load, even in the marrow, without any apparent contact with compact bone.

By the use of histomorphometric data, some estimate of the interfacial shear strength in torsion can be calculated with the following formulae:

$$\tau_b = \frac{M_b/r}{A_T(\%bc)} \quad (1)$$

$$\tau_m = \frac{M_m/r}{A_T(\%bc)} \quad (2)$$

where τ_b = interfacial shear stress in torsion at breakpoint, τ_m = interfacial shear stress in torsion at maximal torque, M_b = break point torque, M_m = maximal torque, r = mean thread radius, A_T = total fixture surface area and %bc = percentage of A_T in direct contact with bone. The results of these calculations are given in *Table 1*. To estimate a shear modulus in torsion, G_t, the thickness of the interface must be known[10]. There is some information about the geometry and the topography of the interface in the thesis by Sennerby[11], indicating an amorphous tissue layer with a thickness of 100–400 nm closest to the titanium oxide, continuing outwards with increasing number of collagen filaments and increased mineralization. Suppose that the interface thickness is i, then:

$$G_t(i) = \frac{\tau_b i}{2\pi r \frac{\phi_b}{360}} \quad (3)$$

where ϕ_b = angular deformation at break point. The results are given in *Table 1*, where the interface thickness was assumed to be 100 and 1000 nm, respectively.

For the pull-out tests, any approximate theory will probably be less realistic than the simple shear stress computation in torsion. For the pull-out test, an average shear stress can be readily computed using a cylinder with a diameter equal to the outer diameter of the threads and a length equal to the axial length of the part of the fixture intended for integration in bone. A better assumption may be to use an effective length instead of the length of the fixture. This effective length could be calculated as the bone thickness multiplied by the relative amount of bone present in the area surrounding the threads. The shear stress in pull-out, τ_p, can then be estimated:

$$\tau_p = \frac{F}{2\pi r_o h(\%ba)} \quad (4)$$

where F = maximal pull-out load, r_o = outer fixture radius, h = bone thickness and %ba = fraction occupied by bone of the area where the load is transferred from the fixture to the bone tissue. The bone thickness, h, and the percentage bone area, %ba, in this formula can be approximated by the measured bone thickness at 50 μm distance from the outer edge of the threads (t_{50}). A shear modulus in pull-out, G_p, can also be estimated assuming that the shear occurs in the space between the outer edge of the threads and the hollow hemisphere that supports the bone (*Figure 3*):

$$G_p = \frac{\tau_p}{\frac{\varepsilon}{r_h - r_o}} \quad (5)$$

where ε = extension or deformation at maximal pull-out load and r_h = radius of the hole in the hemisphere. The results are given in *Table 1*. These results are regarded primarily as a measure of the surrounding bone quality and efficiency of the screw thread design in transferring axial load.

For the torsional shear stress at break point, there was a tendency ($P < 0.10$) to higher values on the right side (*Table 3*). No statistically significant differences were found between the right and left sides for shear stresses and shear moduli in pull-out.

DISCUSSION

The choice of animal model is not evident *a priori* when studying different biomechanical issues[12]. The finding of an early plastic deformation in torsion in the present study seems to be a general finding in every species studied so far with this experimental set-up[4–7]. Therefore, the present rat model may be regarded as a suitable experimental model for evaluation of interface biomechanics of bone-anchored implants. The rat has other advantages, for instance with respect to ethical considerations and handling.

The present morphological evaluation showed that healing of bone around threaded titanium fixtures inserted in the rat cortical bone essentially followed a pattern similar to that described for rabbit cortical bone[13]. After 4 weeks, both remodelling of the interface within the threads and endosteal and periosteal formation of woven bone were prominent findings. After 8 and 16 weeks, a large amount of compact bone was in contact with the implant surface and filled the threads. Although remodelling of the cortical layer was observed in some specimens examined after 4 weeks, an extensive remodelling of the cortex between the inserted fixtures was a major observation after 8 and 16 weeks.

Recent morphological observations[13] in rabbit cortical bone showed that after an initial press-fit contact, bone resorption and remodelling occurred in the interface to fluoroapatite- and hydroxyapatite-coated Ti6Al4V and non-coated commercially pure titanium cylindrical implants. Irrespective of implant material, a (temporary) reduction in bone–implant contact was observed between 3 and 28 days. Although the detailed kinetics during this phase of early healing were not included in the present study, it was evident that bone resorption and formation of new woven bone occurred simultaneously within the threads of the fixture after 4 weeks. It is therefore likely that the period between insertion and 4 weeks is a critical phase in terms of implant stability. It may be argued that the drilling and pre-tapping procedure, together with the threaded design and the surgical installation procedure in the present study, provided stability for encapsulation of the fixture in bone. There was an increase in bone thickness up to 4 weeks, by the formation of new bone above and below the original compacta. This bone is expected to originate from the periosteum and endosteum. Moreover, endosteal bone formation extended along the surface of the threads originally located in the bone marrow. This observation could explain the relatively greater increase in bone thickness close to the fixture (t_{50}), in comparison with the more distant regions (t_{250}, t_{550}). After 16 weeks, extensive remodelling was seen in the cortical layer between the fixtures. At this point of time new bone formation was diminished. The observed reduction in new bone formation and the increase in remodelling might explain the relatively smaller increase in bone thickness between 4 and 16 weeks (*Figure 9*).

Previous investigations have shown an increasing removal torque with time[14], when unscrewing titanium fixtures inserted in the rabbit tibia. The present study reports increasing torsional and pull-out values with time in the rat tibia. In addition, it was possible to identify a pattern of plastic deformation in torsion. This plastic deformation was found both immediately after installation, when no healing could have occurred, and at every time measured. As explained in the Results section, plastic deformation is used here to indicate that, when unloading, there remained an angular displacement rather than a return to the initial zero angle. Plastic deformation was observed even for very small torques, well below the break point (*Figure 6*). No qualitative changes in the interface behaviour could be observed during healing with the test set-up. This indicates that the interface mechanics can be at least partly described by the a model with only bone apposition, without any mechanical bonds between the bone tissue and the titanium fixture surface. Mechanical interlocking at the interface at the microscopical level and friction may contribute to the early plastic deformation observed in torsion. The surfaces of the fixtures used in this study have a certain roughness, deliberately produced, of the order of 5–10 μm in height. The peaks of this roughness may plough through the bone in contact with the fixture to produce the plastic-like behaviour. In pull-out, a linear deformation pattern was observed up to the break point.

The observation of a lag time during the initial 4 weeks until the torsional capacity started to increase corresponds to the initial critical period of bone integration of an implant during healing between days 3 and 28 in the rabbit tibia, based on quantitative morphological data from Dhert *et al.*[13]. The morphological observations in our study indicated that this phase was related to installation trauma, inflammation and removal of injured bone tissue in the interface. The delayed increase in torsional capacity (in comparison with pull-out) might be due to a balance between interfacial resorption and new bone formation.

The increase in bone thickness (t_{250}, t_{550}) around the fixture might be related to the favourable bone-forming conditions in the space created around the fixture, above the cortex and below the surrounding soft tissues, filled with blood, and possibly some stem cells migrating from the marrow and osteogenic cells from the periosteum. The greater increase in bone thickness close to the fixture (t_{50}) was mainly due to endosteal new bone formation. The failure zone in pull-out as observed by fracture lines in the vicinity of the outer part of the threads is located in the region with increased bone thickness[7]. It is reasonable to assume that rapid increase in bone thickness could result in a corresponding increase in pull-out.

The presented rat model may be used for matched investigations, since the majority of measurements were equal on both sides. The observed differences between the right and left sides for some histological parameters do not lend themselves to immediate explanation. Additional observations are necessary to prove whether this is pure coincidence or if the animals use their right and left legs differently.

CONCLUSIONS

During the initial healing phase, the mechanical capacity in pull-out has been shown to have a more rapid increase than the capacity in torsion, indicating

a more pronounced effect of the installation procedure on the bone tissue close to the fixture surface. A correlation was found between mechanical capacity and healing time, and between mechanical capacity and the amount of bone in the interface region.

Shear stresses and shear moduli in torsion and in pull-out were calculated. The healing time did not seem to alter the magnitude of these parameters under the prevailing experimental conditions.

ACKNOWLEDGEMENTS

The technical assistance of A.-K. Blomgren, L. Emanuelsson, C. Morenuis and Y. Winsnes Johansson is greatly appreciated. The study was supported by financial grants from the Swedish Medical Research Council (9495), NUTEK, the King Gustaf V 80-year Fund, the Swedish National Association against Rheumatism, Handlaren Hjalmar Svenssons Research Fund, the Jubileumsklinikens Research Fund against Cancer, and the Swedish Dental Society Research Fund. Illustrations were made by Fredrik Johansson.

REFERENCES

1. Brånemark, P.-I., Hansson, B. O., Adell, R. *et al.*, *Osseointegrated Implants in the Treatment of the Edentulous Jaw. Experience from a 10-year Period.* Almqvist & Wiksell, Stockholm, 1977.
2. Adell, R., Eriksson, B., Lekholm, U., Brånemark, P.-I. and Jemt, T., A long-term follow-up study of osseointegrated implants in the treatment of the totally edentulous jaw. *Int. J. Oral Maxillofac. Impl.*, 1990, **5**, 347–359.
3. Tjellström, A., Osseointegrated systems and their applications in the head and neck. *Adv. Otolaryng. Head Neck Surg.*, 1989, **3**, 39–70.
4. Brånemark, R., Linder, L., Carlsson, Å, Öhrnell, L.-O. and Nilsson, P., Biomechanical characterization of osseointegration in osteoarthritis and rheumatoid arthritis. An experimental *in vivo* investigation in man. Submitted, 1996.
5. Brånemark, R., Öhrnell, L.-O., Skalak, R., Carlsson, L. and Brånemark, P.-I., Biomechanical characterization of osseointegration. An experimental *in vivo* investigation in the beagle dog. Submitted, 1996.
6. Brånemark, R. and Thomsen, P., Biomechanical and morphological studies on osseointegration in immunological arthritis in rabbits. *Scand. J. Plast. Reconstr. Surg. Hand Surg.*, 1997, in press.
7. Öhrnell, L.-O., Brånemark, R., Nyman, J., Nilsson, P. and Thomsen, P., Effects of irradiation on the biomechanics of osseointegration. An experimental *in vivo* study in rats. *Scand. J. Plast. Reconstr. Surg. Hand Surg.*, 1997, in press.
8. Brånemark, R. and Skalak, R., An *in vivo* method for biomechanical characterization of bone anchored implants. Submitted, 1996.
9. Bradley, J. V., *Distribution-free Statistical Tests.* Prentice-Hall, London, 1968, pp. 68–86.
10. Nordin, M. and Frankel, V. H., eds, Biomechanics of bone. *Basic Biomechanics of the Musculoskeletal System*, 2nd edn. Lea & Febiger, Philadelphia, 1989.
11. Sennerby, L., On the bone tissue response to titanium implants. Thesis, Göteborg University, 1991.
12. Koeneman, J., Lemons, J., Ducheyne, P. *et al.*, Workshop on characterization of calcium phosphate materials. *J. Appl. Biomater.*, 1990, **1**, 79–90.
13. Dhert, W. J. A., van Duyn, E., Thomsen, P., Blomgren, A.-K., Verbout, A. J. and Ericson, L. E., Early healing of implants follows different mechanisms for trabecular and cortical bone. 5th Conference of the European Orthopaedic Research Society, 1995.
14. Johansson, C. and Albrektsson, T., Integration of screw implants in the rabbit: a 1-yr follow-up of removal torque of titanium implants. *Int. J. Oral Maxillofac. Impl.*, 1987, **2**, 69–75.